2014

# Tilted femtosecond pulses for velocity matching in gas-phase ultrafast electron diffraction

Ping Zhang
*University of Nebraska–Lincoln*, pzhang4@unl.edu

Jie Yang
*University of Nebraska–Lincoln*, s-jyang6@unl.edu

Martin Centurion
*University of Nebraska-Lincoln*, martin.centurion@unl.edu

Tilted femtosecond pulses for velocity matching in gas-phase ultrafast electron diffraction



2014 New J. Phys. 16 083008

(http://iopscience.iop.org/1367-2630/16/8/083008)

New Journal of Physics
The open access journal at the forefront of physics
Deutsche Physikalische Gesellschaft DPG | IOP Institute of Physics

# Tilted femtosecond pulses for velocity matching in gas-phase ultrafast electron diffraction

**Ping Zhang, Jie Yang and Martin Centurion**
Department of Physics and Astronomy, University of Nebraska–Lincoln, Theodore Jorgensen Hall, 855 N 16th Street Lincoln, NE 68588, USA
E-mail: martin.centurion@unl.edu

Received 21 March 2014, revised 28 May 2014
Accepted for publication 27 June 2014
Published 4 August 2014
*New Journal of Physics* **16** (2014) 083008
doi:10.1088/1367-2630/16/8/083008

## Abstract
Recent advances in pulsed electron gun technology have resulted in femtosecond electron pulses becoming available for ultrafast electron diffraction experiments. For experiments investigating chemical dynamics in the gas phase, the resolution is still limited to picosecond time scales due to the velocity mismatch between laser and electron pulses. Tilted laser pulses can be used for velocity matching, but thus far this has not been demonstrated over an extended target in a diffraction setting. We demonstrate an optical configuration to deliver high-intensity laser pulses with a tilted pulse front for velocity matching over the typical length of a gas jet. A laser pulse is diffracted from a grating to introduce angular dispersion, and the grating surface is imaged on the target using large demagnification. The laser pulse duration and tilt angle were measured at and near the image plane using two different techniques: second harmonic cross correlation and an interferometric method. We found that a temporal resolution on the order of 100 fs can be achieved over a range of approximately 1 mm around the image plane.

Keywords: tilted laser pulse, ultrafast electron diffraction, velocity matching

## 1. Introduction

Recent improvements in electron pulse technology have resulted in tabletop sources capable of delivering femtosecond pulses to a target [1, 2]. This has enabled ultrafast electron diffraction (UED) experiments on solid samples with a resolution on the order of 200 fs [2]. In these experiments, thin (submicrometer) samples were used to capture diffraction patterns in transmission mode. Another important application of UED is investigating ultrafast chemical reactions on isolated molecules. For these experiments, the target is a gas beam with a diameter typically between 0.1 and 1 mm. The group velocity mismatch between the laser and electrons results in a blurring of the resolution as the pulses traverse the gas jet [3]. The group velocity mismatch limits the resolution of most experiments to several picoseconds [4–6], with the highest resolution of 850 fs achieved using a microjet with a diameter of only 0.1 mm [7]. A laser pulse with a tilted intensity front was used to match the velocity of the laser and electrons on the surface of a solid sample [8]. However, the matching has only been demonstrated at a single plane along the propagation direction; therefore, it is not clear that it can be applied to the problem of gas UED, in which the target is extended. For example, electrons with a kinetic energy of 100 keV travel with a speed of 0.55 c, where c is the speed of light in vacuum. A laser pulse propagating at an angle of 57° with respect to the electron beam, with a pulse front tilted at the same angle, would match the speed of the electrons. However, the problem is that the velocity must be matched throughout the length of the gas target and both the tilt angle and duration of the laser pulse change as it propagates. In this paper, we investigate this issue in detail and show experimentally that, with the appropriate optical design, it is possible to achieve a resolution on the order of 100 fs.

A tilted laser pulse has an intensity front that is tilted with respect to the direction of propagation. The component of the laser group velocity in the direction normal to the intensity front depends on the tilt angle [9]. This dependence can be exploited to match the normal laser velocity to the velocity of either the electrons or the electromagnetic waves traveling more slowly through a medium. Several applications of tilted pulses have been reported in the literature. Tilted pulses have also been used to match the group velocity of a pump laser to the phase velocity of terahertz waves to increase the efficiency of optical rectification [10–12]. In x-ray laser generation, a tilted laser front—generated by step mirrors or a slightly misaligned laser compressor—was used to provide optimum preplasmas for a traveling wave pumped by a second laser pulse [13–15]. The angular dispersion used to generate a tilted pulse front also results in a rotation of the pulse front as the beam focuses and defocuses [16, 17]. Femtosecond laser pulses with such rotating fronts have been used recently for electron wakefield acceleration and the generation of attosecond pulses [18–20].

For gas-phase UED experiments, the laser beam is focused to a spot size below 0.5 mm to achieve high fluence and minimize the group velocity mismatch. Thus, in addition to a large tilt angle, a large demagnification factor is required. In our configuration, a grating provides the angular dispersion. The grating surface is imaged onto the target with a demagnification factor ($M$) of 12.7. At the image plane, the diffracted components will recombine into a short pulse, as long as the diffracted beam is normal to the grating surface. However, a longer pulse duration is expected both before and after the image plane. We use an optical setup with a long Rayleigh length, about 2 mm, to lessen the broadening of the pulse duration as it traverses the target. Optical aberrations might also result in increased pulse duration across the beam, even at the image plane. For gas-phase UED experiments, the pulse duration must remain short over the

length of the target. We measured the tilt angle and pulse duration as a function of the distance from the image plane and at several positions laterally across the beam. We used a simple technique that consists of measuring the interference between the tilted pulse and a known reference pulse [21]. These results have been compared to those from a previously demonstrated technique using second harmonic generation (SHG) between the tilted pulse and a reference pulse [22]. The interferometric technique is more convenient for *in situ* measurements because it requires only a detector (or screen) to be placed at the position of the measurement.

## 2. Theory

A laser pulse with a tilted front can be generated by propagation through a prism [23, 24] or diffraction from a grating [24]. In the case of diffraction from a grating, the tilt angle $\gamma$ is given by [22, 24]

$$\gamma = \arctan\left[\Psi\lambda_0\right] \tag{1}$$

where $\Psi = M\left(\frac{d\theta_{out}}{d\lambda}\right)_{\lambda_0}$ is the angular dispersion, $\theta_{out}$ is the angle of the diffracted beam with respect to the grating normal, $\lambda_0$ is the central wavelength of the laser pulse, and $M$ is the demagnification factor. If no demagnification is involved, $M$ will be 1. The angular dispersion depends on the diffracted order and the grating constant

$$\left(\frac{d\theta_{out}}{d\lambda}\right)_{\lambda_0} = \frac{kd}{\cos\ \theta_{out}} \tag{2}$$

where $d$ is the grating constant and $k$ is the diffraction order. In our experiments, we used the first-order diffracted beam ($k = 1$).

If the beam is demagnified using imaging optics, $M$ is a function of position and is given by the ratio of the diameter of the laser beam on the grating to the diameter of the laser beam at the position where the tilt is measured. The angular dispersion $\Psi$ generated by the grating results in a temporal chirp such that pulse duration increases as the pulse propagates away from the grating. The pulse duration $\tau$ at a distance $z$ from the grating is given by

$$\tau(z) = \tau_0\sqrt{1 + \frac{(2\ \ln\ 2)^2 z^2 \lambda_0^6}{\pi^2 c^4 \tau_0^4}\Psi^4} \tag{3}$$

where $\tau_0$ is the original laser pulse duration (60 fs in our experiments) [17, 22]. To recreate a short pulse at a target position, the grating surface must be imaged at this position. It has been shown that a nonzero value for $\theta_{out}$ will result in temporal aberrations [22], as the distance to the image plane will be different across the beam. The requirement of $\theta_{out} = 0$ prevents us from using the experimental setup shown in references [15, 18]. In [22], the pulse duration on the image plane was measured for $M = 1$. Here, we investigate the case of large demagnification and measure the pulse duration both across the beam and as a function of distance to the focal plane.

## 3. Experimental setup

Figure 1 shows the experimental setup used to generate and measure the tilted pulses. The tilt angle and pulse duration were measured using a cross correlation between the tilted pulse and a

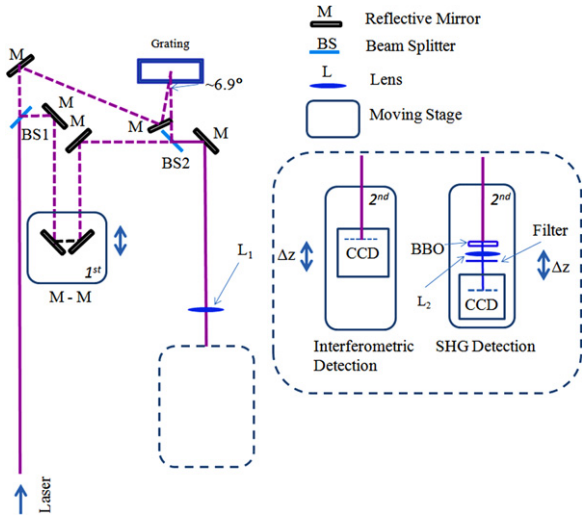


**Figure 1.** Sketch of the experimental setup for tilted front laser pulse generation and measurement. The first moving stage was used to control the delay time between the reference laser and the tilted front laser. The second moving stage is in the detection part and controls the shift $\Delta z$ with respect to the image plane.

(nontilted) reference pulse using SHG or by directly measuring the interference between the two pulses. For the SHG method, the two pulses overlapped in a thin barium borate (BBO) crystal placed at the image plane (see inset in figure 1). Due to the tilt in one of the pulses, the two pulses spatially overlapped only along a narrow strip. The width of the spatial overlap region depended upon the duration of the pulses. A second harmonic signal was generated in the region where the two pulses overlapped. This region was imaged on a charge-coupled device (CCD) camera, while light at the fundamental frequency was blocked with a filter. The tilt angle was measured by recording the horizontal shift in the overlap region as a function of the delay of the reference pulse. The BBO crystal and CCD were translated together along the direction of the optical beam to measure the tilt angle and pulse duration as a function of distance from the image plane. For the interferometric measurement, the CCD camera was placed directly at the position where the pulses overlapped. Instead of measuring the width of the region where SHG was observed, the region of interference was measured directly.

The laser system delivered 60 fs pulses at a central wavelength of $\lambda_0 = 800$ nm and pulse energy of 2 mJ with a repetition rate of 5 kHz. The laser beam was attenuated and then evenly split into two beams with a polarizing beam splitter (BS1 in figure 1). One beam was diffracted from a reflection grating to introduce angular dispersion. The laser beam incident on the grating was slightly elliptical with a full width at half maximum (FWHM) of 7.0 mm in the vertical direction and 6.0 mm in the horizontal direction.

The diffraction grating was a gold-coated holographic grating with a grating constant of $d = 150\,\mathrm{mm}^{-1}$. This small grating constant was used to achieve the desired angular tilt with a large demagnification factor. Using the grating formula, $(\sin\theta_{in} + \sin\theta_{out}) = d\lambda_0$, we calculated that an incident angle of $\theta_{in} = 6.9°$ would result in the diffracted beam being normal to the grating surface. In this configuration, the diffraction efficiency of the grating into the first order was 80%. The reference beam traveled through a variable delay line to adjust the time of arrival at the BBO crystal. Both beams were focused onto the BBO with a 23 cm focal

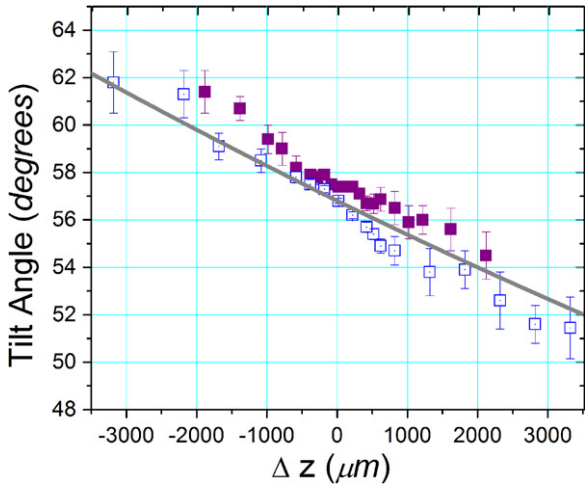


**Figure 2.** Tilt angle as a function of distance from the image plane. The dark grey line is the calculation result, blue open squares are the values measured using the SHG technique, and the purple filled squares are the results from the interferometric measurement.

length lens ($L_1$). The distance between the grating and the lens was $S_0 = 315$ cm. Using the lens maker's equation, $1/S_0 + 1/S_i = 1/f$, we found that the distance from the lens to the image plane was $S_i = 24.8$ cm. The demagnification factor was $M = \phi_0/\phi_i = S_0/S_i = 12.7$, where $\phi_0$ and $\phi_i$ are the laser beam diameters on the grating and on image plane, respectively. The beam size on the image plane was elliptical with FWHM of 0.56 and 0.47 mm. The tilt angle ($\gamma$) was 56.8°. The value of $M$ (and thus the tilt angle) could be adjusted to match electron pulses with different kinetic energies by changing the distances. The BBO crystal used for SHG had a thickness of 0.20 mm. A FGB39 band pass filter was used to block the fundamental wave and transmit the second harmonic. The surface of the BBO crystal was imaged using lens $L_2$ (2.4 cm focal length) onto a CCD detector with four times magnification. Data were recorded for several positions before and after the image plane by moving the BBO crystal, lens $L_2$, and the detector together along the direction of beam propagation for the SHG measurements. For the simpler interferometric measurements, only the detector position had to be varied. A small vertical angle was introduced between the tilted and reference pulses that created interference fringes. The pulse duration was also measured at five different positions across the beam by changing the delay between the pulses.

## 4. Experimental results and discussion

### *4.1. Tilt angle*

Figure 2 shows the measured tilt angle versus the displacement from the image plane $\Delta z$ in the region near the image plane, where $\Delta z = z_{L1} - S_i$ and $z_{L1}$ is the either distance from lens $L_1$ to the detector in the interferometric method or to the BBO crystal in the SHG method. The experimental results from the interferometric and SHG techniques are in good agreement. The tilt angle decreased with increasing $\Delta z$ because the beam diameter was increasing. The minimum beam diameter occurs before the image plane. The zero of $\Delta z$ was defined as the

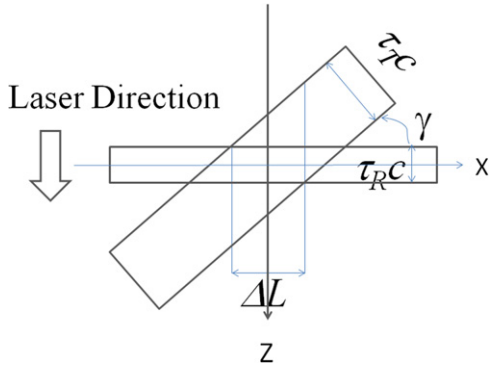


**Figure 3.** Sketch of the overlap of tilted and reference pulses.

position where the pulse duration was minimized. The dark grey line in figure 2 shows the tilt angle calculated using equation (1) applied to the image plane, where $\Delta z$ replaces $z$ and $d_i = Md = 12.7d$ replaces $d$. We treat the light field on the image plane as an image of the light field immediately leaving the grating, such that the phase modulation imprinted by the grating on the beam has a spatial frequency increased by a factor of $M$.

Assuming a Gaussian beam away from the focus, the divergence angle ($\alpha$) after the focal plane can be approximated by $\tan(\alpha/2) = \frac{R(\Delta z)}{S+\Delta z}$, where $S = 1.8$ cm is the distance from the focal plane to the image plane and $R(\Delta z)$ is the laser beam radius as a function of $\Delta z$. We expect this to be a good approximation because $S$ is significantly larger than the Rayleigh length (2 mm). The demagnification relative to the beam size at the image plane is $M_i(\Delta z) = \frac{R_i}{R(\Delta z)} = \frac{S}{S+\Delta z}$, where $R_i$ is the radius of the beam at the image plane. The tilt angle near the image plane is

$$\gamma(\Delta z) = \arctan\left(M_i(\Delta z) d_i \lambda_0\right) = \arctan\left(\frac{S}{S+\Delta z} d_i \lambda_0\right). \tag{4}$$

There is good agreement between the theoretical and experimental results. The plotted line in figure 2 corresponding to the theory does not include any fitted parameters. The measured tilt angles from the interferometric method are consistently larger than those measured with the SHG method. We attribute this to the uncertainty in finding the position of the image plane (position 0 in figure 2). This uncertainty is on the order of $\pm 200\,\mu$m for the interferometric method. With the SHG method, the position of the image plane can be determined more accurately because the overlap region is imaged onto the CCD with magnification. For $\Delta z$ values that are small compared to $S$, the tilted angle ($\gamma$) varies at a rate of approximately $-1.5°$/mm. A change in tilt angle on the order of 1° would not significantly affect the velocity mismatch or temporal resolution of the experiment. For example, if the tilt angle were off by 1°, the velocity difference would be only $0.015\,c$.

### *4.2. Pulse duration*

In the SHG measurement, the pulse duration ($\tau_T$) of the tilted pulse was obtained from the FWHM of the spatial overlap of the two beams $\Delta L$ (figure 3),

$$\tau_T = \left( \frac{\Delta L}{c} \sin \gamma + \tau_R \cos \gamma \right) \tag{5}$$

where $\tau_R$ is the pulse duration of the reference pulse.

The tilted pulse duration $\tau(\Delta z)$ at different positions can be deduced from $\tau_T \approx \sqrt{\tau(\Delta z)^2 + \tau_R^2 + \tau_{camera}^2}$ [22]. Here, $\tau_{camera}$ depends on the pixel size of the CCD camera. Our camera has a pixel size of 5.2 $\mu$m, corresponding to a temporal resolution of $\tau_{camera} = 5.2\,\mu m \tan[\gamma(\Delta z)]/c$.

For the interferometric method, $\tau_T$ can also be extracted from the measured width of the interferometric cross correlation ($\Delta L$). Assuming that the beams have a Gaussian temporal profile, the electric fields of the reference ($\varepsilon_R$) and tilted ($\varepsilon_T$) pulses at a specific $z$ coordinate can be written as

$$\varepsilon_R = e^{-\alpha_R t^2} e^{i\omega_0 t};\ \varepsilon_T = e^{-\alpha_R t'^2} e^{i\omega_0 t} \tag{6}$$

where $\alpha_R = 2\ln 2/\tau_R^2$, $\alpha_T = 2\ln 2/\tau_T^2$, $t$ is time, $\omega_0$ is the central frequency, and $t' = t - \frac{x}{c}\tan\gamma$ describes the time delay of the tilted pulse front. The interference intensity at the detector is

$$I = \int_{-\infty}^{\infty} \left|\varepsilon_R + \varepsilon_T\right|^2 dt = \int_{-\infty}^{\infty} \left|\varepsilon_R\right|^2 dt + \int_{-\infty}^{\infty} \left|\varepsilon_T\right|^2 dt + \int_{-\infty}^{\infty} \varepsilon_R^* \varepsilon_T dt + c.c \tag{7}$$

where c.c. denotes the complex conjugate. The first and second terms make a constant contribution ($C_0$) to laser intensity, whereas the third and fourth terms represent interference.

Substituting equation (6) into equation (7), we obtain

$$\begin{aligned} I &= C_0 + C_1 \exp\left( -\frac{\alpha_R \alpha_T}{\alpha_R + \alpha_T} \frac{x^2}{c^2} \tan^2\gamma \right) \\ &= C_0 + C_1 \exp\left( -\frac{2\ln 2}{\tau_R^2 + \tau_T^2} \frac{x^2}{c^2} \tan^2\gamma \right) \end{aligned} \tag{8}$$

where $C_1$ is a constant. The interference has a Gaussian shape with FWHM given by

$$\frac{\Delta L}{c} = \frac{\sqrt{2\left(\tau_R^2 + \tau_T^2\right)}}{\tan\gamma} \quad or \quad \tau_T = \sqrt{\frac{\left(\frac{\Delta L}{c}\right)^2 \tan^2\gamma}{2} - \tau_R^2} \tag{9}$$

Figure 4 shows the experimental and calculated pulse widths [$\tau_T$ ($\Delta$z)] over a region of approximately 3 mm before and after the image plane. There is good agreement between both experimental methods, and between the experiment and theory. The calculation was completed using equation (3) with the displacement and tilted angle as described in section 4.1. The pulse duration reaches a minimum of 66 fs at the image plane, compared to the initial pulse duration of 60 fs. The small broadening of the pulse duration maybe be due to aberrations or dispersion in the optical system. The pulse duration increases to 300 fs at a distance of 3 mm after the image plane. The pulse duration increases more rapidly for displacements toward the focus because the beam diameter becomes smaller and thus, the tilt angle and dispersion are larger.

At each position, the pulse duration was measured at five lateral positions across the beam, and it was found to vary by approximately 5% across the beam with the minimum near the beam center, which means that aberrations do not cause significant broadening transversely in

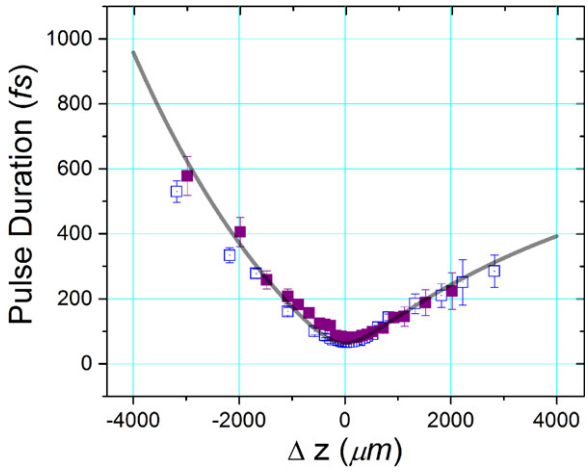


**Figure 4.** Pulse duration of tilted pulse as a function of the displacement Δz from the image plane. The black line is the calculated pulse duration. The blue open squares are the values measured using the SHG method and the purple filled squared are the values measured with the interferometric method.

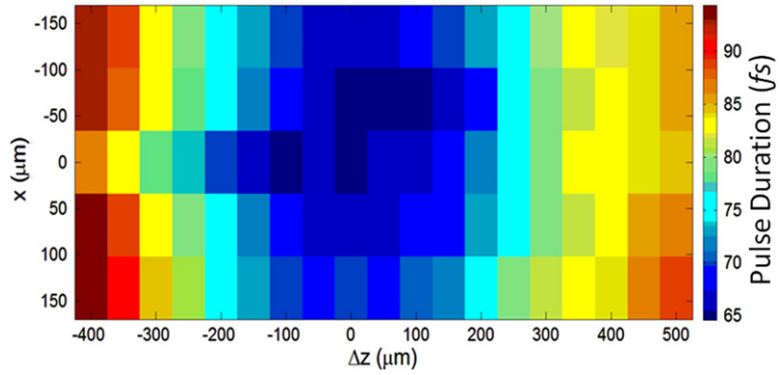


**Figure 5.** Pulse duration versus displacement $\Delta z$ from the image plane and transverse position x across the beam. Position x originated around the center of the laser beam.

our configuration. Figure 5 shows the pulse duration as a function of the lateral position from the beam center and as a function of distance for a region near the image plane.

### *4.3. Damage threshold of grating*

The full characterization of the pulse duration and the good agreement with theory give us confidence that this method can be applied successfully to UED and other experiments. With the current setup, the main limitation to the intensity that can be reached at the target (the image plane) is the damage threshold of the grating. A tighter focusing geometry would lead to higher intensity, but would also result in a reduced Rayleigh length that would make it more difficult to have velocity matching over an extended target. Thus, the best way to increase the intensity is to keep the same configuration but reduce the size of the beam incident on the grating. To determine how far the intensity could be increased with our current configuration, we measured the damage threshold of the grating.

The laser pulse was focused to an area of $4.5 \times 10^{-3}$ cm$^2$ on the grating. The grating surface was imaged on a CCD camera with three times magnification. The pulse energy was increased in small steps and the grating was exposed to the laser for 40 min at each step. Damage was defined as any change in the diffracted laser beam. For a pulse energy of 0.54 mJ, a damaged spot was observed after 2 min of irradiation. For an energy of 0.50 mJ, a damage spot was visible after approximately 40 min. For a pulse energy of 0.40 mJ, no damaged was observed even after 2 h of irradiation. Thus, we conclude that the grating can be safely operated at a fluence of 90 mJ cm$^{-2}$, with the damage threshold at or below 110 mJ cm$^{-2}$. For a pulse duration of 60 fs, safe operation would mean a maximum intensity of $1.5 \times 10^{12}$ W cm$^{-2}$ on the grating and $2.4 \times 10^{14}$ W cm$^{-2}$ on the image plane.

### *4.4. Implication for gas-phase UED experiments*

Our results indicate that it is be possible to reach a temporal resolution on the order of 100 fs for gas-phase UED experiments using tilted laser pulses to compensate for the group velocity mismatch. For example, let us consider the broadening that can be expected for a typical gas jet with a diameter between 0.5 and 1 mm. For a UED experiment without pulse tilting, the velocity mismatch would limit the resolution to several picoseconds [25]. With pulse tilting, there are two contributions to the broadening: the increase in the laser pulse duration and the remaining velocity mismatch due to the change in the tilt angle of the laser as it traverses the target. In our measurements, we started with a laser pulse duration of 60 fs at the output of the laser, and measured a pulse duration of 66 fs at the image plane of the grating. The average pulse duration over a 0.5 mm distance around the image plane was 71 fs, and it increased to 78 fs when averaged over 1 mm. For the effect of the remaining velocity mismatch, we consider that the angle changes at a rate of 1.5°/mm. If the tilt angle is off by 1°, the velocity mismatch between the laser and the electrons will be $0.015\,c$. This will lead to a broadening of the resolution of about 60 fs mm$^{-1}$. The total resolution of the experiment can be calculated as $T_{total}^2 = t_{Laser}^2 + t_{GVM}^2 + t_{Electron}^2$, where the three terms on the right represent the laser pulse duration, broadening due to group velocity mismatch, and the electron pulse duration, respectively. For an electron pulse duration of 100 fs, the overall temporal resolution will be 126 fs for a target diameter of 0.5 mm and 140 fs for a target diameter of 1 mm. For longer electron pulses, the resolution will be determined mainly by the electron pulse duration. If shorter electron pulses are available, a resolution of 50 fs is within reach by using shorter laser pulses and keeping the target diameter below 0.5 mm.

In many photochemistry experiments, the photon energy required for excitation is in the ultraviolet range. Here, we discuss how changing the wavelength will affect the overall time resolution. Take the third harmonic, $\lambda = 267$ nm, as an example. To keep the tilt angle the same, the grating constant $d$ must be tripled to compensate for the wavelength change, according to equations (1) and (2). Substituting this change into equation (4), we obtain that the tilt angle variation around the image plane will be the same as for the 800 nm pulse. The change in the pulse duration is described by equation (3), where the wavelength dependent term inside the square root is proportional to $\lambda^6\Psi^4$ or $\lambda^6 d^4$. Thus, at the shorter wavelength, the spreading in the pulse duration will be less severe if the same tilt angle is used. Therefore, the time resolution broadening due to the variation of the tilt angle around the image plane will be independent of wavelength, whereas the broadening due to pulse duration will be reduced for shorter wavelengths.

## 5. Conclusion

We experimentally studied the generation and measurement of a high-intensity tilted front femtosecond laser pulse for velocity matching in UED experiments. The tilted pulse was generated by imaging the surface of a diffraction grating onto the target position. We measured the tilted angle and pulse duration in the range of ±3 mm around the image plane using the SHG method and an interferometric method. The interferometric method is better suited for *in situ* measurements, as it requires only a measurement of the interference pattern at the target position. With an input pulse duration of 60 fs, we measured a pulse duration of 66 fs on the image plane, and the duration stayed below 100 fs for a distance of ±0.5 mm around the image plane. We showed that the pulse duration does not vary significantly across the beam. Our optical configuration is well suited for applications that require a large tilt angle and high fluence, and it can be used to reach an intensity above $10^{14}\,W\,cm^{-2}$ on the image plane while preserving the pulse duration and tilt angle through the target. For UED experiments, tilted pulses could be used in combination with methods to produce femtosecond electron pulses [1, 26, 27] to break the 100 fs resolution barrier in gas-phase experiments.

## Acknowledgment

This work was supported by a grant from the US Air Force Office of Scientific Research (award number FA9550-12-1-0149).

## References

[1] van Oudheusden T, Pasmans P L E M, van der Geer S B, de Loos M J, van der Wiel M J and Luiten O J 2010 Compression of subrelativistic space-charge-dominated electron bunches for single-shot femtosecond electron diffraction *Phys. Rev. Lett.* **105** 264801

[2] Siwick B J, Dwyer J R, Jordan R E and Miller R J D 2003 An atomic-level view of melting using femtosecond electron diffraction *Science* **302** 1382–5

[3] Williamson J C and Zewail A H 1993 Ultrafast electron diffraction. Velocity mismatch and temporal resolution in crossed-beam experiments *Chem. Phys. Lett.* **209** 10–6

[4] Park S T, Gahlmann A, He Y, Feenstra J S and Zewail A 2008 Ultrafast electron diffraction reveals dark structures of the biological chromophore indole *Chem. Int. Ed.* **47** 9496–9

[5] Reckenthaeler P R, Centurion M, Fuss W, Krausz F and Fill E E 2009 Time-resolved electron diffraction from selectively aligned molecules *Phys. Rev. Lett.* **102** 213001

[6] Srinivasan R, Feenstra J S, Tae Park S, Xu S and Zewail A H 2005 Dark structures in molecular radiationless transitions determined by ultrafast diffraction *Science* **307** 558

[7] Hensley C J, Yang J and Centurion M 2012 Imaging of isolated molecules with ultrafast electron pulses *Phys. Rev. Lett.* **109** 133202

[8] Baum P and Zewail A H 2006 Breaking resolution limits in ultrafast electron diffraction and microscopy *Proc. Natl Acad. Sci. USA* **103** 16105–10

[9] Szatmári S, Simon P and Feuerhake M 1996 Group-velocity-dispersion-compensated propagation of short pulses in dispersive media *Opt. Lett.* **15** 1156–8

[10] Hebling J, Almási G, Kozma I Z and Kuhl J 2002 Velocity matching by pulse front tilting for large area THz-pulse generation *Opt. Express* **10** 116–1166

[11] Stepanov A G, Bonacina L, Chekalin S V and Wolf J-P 2008 Generation of 30 $\mu$J single-cycle terahertz pulses at 100 Hz repetition rate by optical rectification *Opt. Lett.* **33** 2497–9

[12] Yeh K-L, Hoffmann M C, Hebling J and Nelson K A 2007 Generation of 10 $\mu$J ultrashort terahertz pulses by optical rectification *Appl. Phys. Lett.* **90** 171121
[13] Daido H 2002 Review of soft x-ray laser researches and developments *Rep. Prog. Phys.* **65** 1513–76
[14] Tommasini R and Fill E E 2001 Effective traveling-wave excitation below the speed of light *Opt. Lett.* **26** 689–91
[15] Chanteloup J-C *et al* 2000 Pulse-front control of 15 TW pulses with a tilted compressor, and application to the subpicosecond traveling-wave pumping of a soft-x-ray laser *J. Opt. Soc. Am.* B **17** 151–7
[16] Akturk S, Gu X, Zeek E and Trebino R 2004 Pulse-front tilt caused by spatial and temporal chirp *Opt. Express* **12** 4399–410
[17] Osvay K 2004 Angular dispersion and temporal change of femtosecond pulses from misaligned pulse compressors *IEEE Journal of Selected Topics in Quantum Electronics* **10** 213–20
[18] Popp A *et al* 2010 All-optical steering of laser-wakefield-accelerated electron beams *Phys. Rev. Lett.* **105** 215001
[19] Wheeler J A, Borot A, Monchocé S, Vincenti H, Ricci A, Malvache A, Lopez-Martens R and Quéré F 2012 Attosecond lighthouses from plasma mirrors *Nature Photons* **6** 829–33
[20] Kim K T, Zhang C, Ruchon T, Hergott J-F, Auguste T, Villeneuve D M, Corkum P B and Quéré F 2013 Photonic streaking of attosecond pulse trains *Nature Photons* **7** 651–6
[21] Bor Z, Gogolak Z and Szabo G 1989 Femtosecond-resolution pulse-front distortion measurement by time-of-flight interferometry *Opt. Letts.* **16** 862–4
[22] Kreier D and Baum P 2012 Avoiding temporal distortions in tilted pulses *Opt. Letts.* **37** 2373–5
[23] Isaienko O and Borguet E 2009 Pulse-front matching of ultra-broad band near-infrared noncollinear optical parametric amplified pulses *J. Opt. Soc. Am.* B **26** 965–72
[24] Bor Z, Rácz B, Szabó G, Hubert M and Hazim H A 1993 Femtosecond pulse front tilt caused by angular dispersion *Opt. Eng.* **32** 2501–3
[25] Dantus M, Kim S B, Charles Williamson J and Zewail A H 1994 Ultrafast electron diffraction. 5. Experimental time resolution and applications *J. Phys. Chem.* **98** 2782–96
[26] Hansen P, Baumgarten C, Batelaan H and Centurion M 2012 Dispersion compensation for attosecond electron pulses *Appl. Phys. Lett.* **101** 083501
[27] Hilbert S A, Uiterwaal C, Barwick B, Batelaan H and Zewail A H 2009 Temporal lenses for attosecond and femtosecond electron pulses *PNAS* **106** 10558–63